Relativistic Study on Emission Mechanism in Palladium and Platinum Complexes

Takeshi Matsushita,[†,‡] Toshio Asada,[†] and Shiro Koseki*[,†]

Department of Chemistry, Graduate School of Science, Osaka Prefecture University, 1-1 Gakuen-cho, Naka-ku, Sakai, Osaka 599-8531, Japan, and Chisso Corporation, 2-2-1 Ootemachi, Chiyoda-ku, Tokyo 100-8105, Japan

Received: May 29, 2006; In Final Form: September 27, 2006

The present study investigates the spin−orbit coupling (SOC) effects in the radiative processes from the electronically excited states of bis-[2-(2-thienyl)-pyridine] platinum ($Pt(thpy)_2$) and palladium ($Pd(thpy)_2$). The transition probabilities among the low-lying spin-mixed states in these complexes are estimated using the discrete variable representation (DVR) method based on the assumption that the system obeys Fermi's golden rule. It is revealed that the low-lying excited singlets and triplets are strongly mixed with each other by SOC in $Pt(thpy)_2$ and, as a result, a fast nonradiative transition occurs to the low-lying excited spin-mixed states. This is followed by the radiative transition from these low-lying spin-mixed states to the lowest spin-mixed state (the ground state); that is to say, a phosphorescence should be observed from these low-lying excited spin-mixed states in $Pt(thpy)_2$. On the contrary, weak SOCs are obtained in $Pd(thpy)_2$ and no phosphorescence at room temperature is expected to be observed in $Pd(thpy)_2$. These results are in good agreement with the experimental reports.

1. Introduction

Much attention has been paid to the photophysical and photochemical properties of the transition metal complexes coordinated by organic ligands, especially in the fields of organic light emitting diodes (OLEDs).[1−16] If both the singlet and triplet excitons generated by electrical pumping can be used for the emission in OLEDs, the internal quantum efficiency (η_{int}) could reach 100%. It is known that, when iridium complexes are employed as the phosphorescent dye, η_{int} is close to 100%.[1,3−5,8,9] It is also suggested that the best efficiency can be obtained if the material is phosphorescent at room temperature. However, such a phosphorescent material has been rarely found since, generally speaking, fluorescence occurs more effectively than phosphorescence because of the spin-allowed transition. For the purpose of obtaining a strong phosphorescence, highly efficient OLEDs must have a strong spin−orbit coupling (SOC) among the low-lying states, since SOC provides a fast intersystem crossing (ISC) between states of different spin multiplicity. Accordingly, heavy metal complexes should be typical candidates as better OLEDs.[17]

Many experimental studies[16,18−32] suggest that cyclometalated Pt(II) complexes might be phosphorescent, since, for instance, bis-[2-(2-thienyl)-pyridine] platinum $Pt(thpy)_2$ has a strong emission from the triplet states at 580 nm in both the photoluminescence (PL)[18−20,30] and electroluminescence (EL)[16,28,33] spectra. Furthermore, Kalinowski et al. recently synthesized several kinds of cyclometalated Pt(II) complexes and reported that their maximum external quantum efficiencies (5.4−11.5%) apparently exceed the limitation of the fluorescent efficiency (5%),[16] where the limitation is derived from the assumption that the singlet excitons of 25% are generated by electric excitation and that the damping (light out-coupling) occurs by passing glass substrate.[9]

To our knowledge, only a few theoretical studies have been performed on the emission mechanisms of phosphorescent transition metal compounds. This is mainly because it is difficult

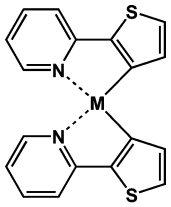

M = Pd, Pt

to electronically characterize excited states in such heavy metal complexes. The recent development of computers and computational technologies has allowed us to calculate large-sized molecules at higher levels of theory. Pierloot et al.[34] characterized excited states in cyclometalated Pd and Pt complexes in detail at the CASSCF/CASPT2 levels of theory and compared the excitation energies with the experimental spectra within adiabatic approximation. Unfortunately, relativistic studies for these complexes have not been performed yet, and it is of special importance to estimate coupling between states of different spin multiplicities, which explain the processes of ISC and phosphorescence.

It is very useful to theoretically examine whether or not newly designed materials are phosphorescent before their syntheses. For this purpose, it is necessary to estimate the transition probability for emission between states of different spin multiplicities (spin-forbidden process), as well as that between states of the same spin multiplicity (spin-allowed process). We have been developing and examining the program codes for estimating the SOC effects in simple transition metal compounds using the MCSCF+FOCI(or SOCI)/SBKJC(f,p) method within the Z_{eff} approximation,[35−40] where MCSCF is the abbreviation for the multiconfiguration self-consistent field method,[41] FOCI is for the first-order configuration interaction,[42] SOCI is the second-order configuration interaction,[42] and SBKJC is the effective core potential basis set proposed by Stevens and coworkers.[43,44] Using this relativistic method, we already reported a comprehensive set of spectroscopic parameters, such as dissociation energies, equilibrium internuclear distances, vibra-

* To whom correspondence should be addressed. E-mail: shiro@c.s.osakafu-u.ac.jp.
† Osaka Prefecture University.
‡ Chisso Corporation.

10.1021/jp0632992 CCC: $33.50 © 2006 American Chemical Society
Published on Web 11/18/2006

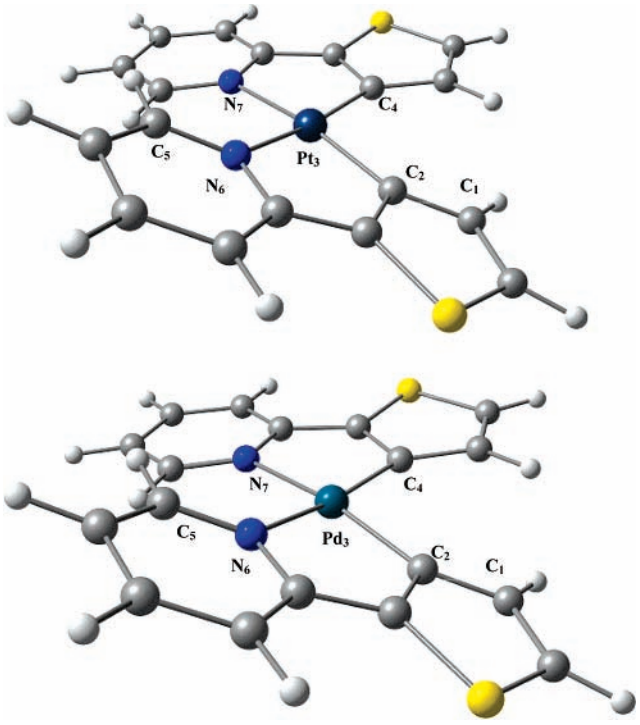

Figure 1. Optimized geometries (C_2 symmetry) for $Pt(thpy)_2$ (top) and $Pd(thpy)_2$ (bottom).

tional frequencies, anharmonicities, and rotational constants, for several transition metal hydrides.[39,40,45]

The purpose of the present study is to theoretically analyze the relaxation mechanisms from the low-lying excited states in Pd and Pt complexes (see Figure 1). The transition probabilities for the emission from the lowest excited singlet and triplet in these complexes are estimated on the basis of the SOC results obtained within the Z_{eff} approximation.[35−40] The present study is the first application of our method to large-sized molecules and provides useful suggestions for designing new phosphorescent OLED materials for industrial production.

2. Methods of Calculation

The SBKJC basis sets[43,44] augmented by a set of polarization functions[46] were used for the transition elements and the second-row main-group elements, and the 31G basis set was used for hydrogen atoms. The geometrical structures of the ground state and the lowest triplet state were optimized using the restricted and unrestricted B3LYP methods,[47] respectively. This method is referred to as B3LYP/SBKJC+p in the following discussion. At these optimized geometries, the MCSCF wave functions were computed for several low-lying singlet and triplet states. Both the experimental and theoretical studies[20−26,29−34,48−52] have reported that low-lying excited states of cyclometalated Pd and Pt complexes are generated by the metal-to-ligand charge-transfer (MLCT) transition, ligand-centered (LC) transition, or their mixture. Therefore, we decided that the MCSCF active space includes five occupied orbitals and two vacant orbitals; the five occupied orbitals have large coefficients of the transition metal d orbitals and the ligands' π orbitals, while the two vacant orbitals have large components of the ligands' π orbitals (Figures 2 and 3). This MCSCF active space can describe both the MLCT and LC states. We also employed a state-averaged (SA) technique during the MCSCF iterations, since the low-lying excited singlet and triplet states, as well as the ground state, need to be described at the same levels of theory. This method is referred to as MCSCF(10,7). The details of the SA-MCSCF calculations are described in section 3.1.

TABLE 1: Relative Energies ΔE [cm^{-1}] of Low-Lying Adiabatic States and Their Main Electron Configurations in $Pt(thpy)_2$ and $Pd(thpy)_2$

	ΔE	electron configuration[a]	coefficient[a]
		$Pt(thyp)_2$	
$S_0(^1A)$	0	$(b)^2(a)^2(b)^2(a)^2(a)^2(b)^0(a)^0$	0.939
$T_1(^3A)$	19 001	$(b)^2(a)^2(b)^1(a)^2(a)^2(b)^1(a)^0$	0.903
$T_2(^3B)$	20 581	$(b)^2(a)^2(b)^2(a)^1(a)^2(b)^1(a)^0$	0.688
		$(b)^2(a)^2(b)^2(a)^2(a)^1(b)^1(a)^0$	0.576
$T_3(^3B)$	21 748	$(b)^2(a)^2(b)^2(a)^1(a)^2(b)^1(a)^0$	0.657
		$(b)^2(a)^2(b)^2(a)^2(a)^1(b)^1(a)^0$	−0.628
$S_1(^1A)$	22 050	$(b)^2(a)^2(b)^1(a)^2(a)^2(b)^1(a)^0$	0.932
$S_2(^1B)$	23 932	$(b)^2(a)^2(b)^2(a)^1(a)^2(b)^1(a)^0$	0.939
$S_3(^1B)$	26 121	$(b)^2(a)^2(b)^2(a)^2(a)^1(b)^1(a)^0$	0.917
		$Pd(thyp)_2$	
$S_0(^1A)$	0	$(a)^2(b)^2(a)^2(b)^2(a)^2(b)^0(a)^0$	0.936
$T_1(^3B)$	22 138	$(a)^2(b)^2(a)^2(b)^1(a)^2(b)^1(a)^0$	0.714
		$(a)^2(b)^2(a)^2(b)^2(a)^1(b)^0(a)^1$	0.590
$T_2(^3A)$	22 153	$(a)^2(b)^2(a)^2(b)^2(a)^1(b)^1(a)^0$	0.717
		$(a)^2(b)^2(a)^2(b)^1(a)^2(b)^0(a)^1$	0.586
$T_3(^3B)$	34 025	$(a)^2(b)^2(a)^1(b)^2(a)^2(b)^1(a)^0$	0.686
		$(a)^2(b)^1(a)^2(b)^2(a)^2(b)^0(a)^1$	0.570
$T_4(^3A)$	34 231	$(a)^2(b)^1(a)^2(b)^2(a)^2(b)^1(a)^0$	0.653
		$(a)^2(b)^2(a)^1(b)^2(a)^2(b)^0(a)^1$	0.608
$S_1(^1B)$	37 183	$(a)^2(b)^2(a)^2(b)^1(a)^2(b)^1(a)^0$	0.706
		$(a)^2(b)^2(a)^2(b)^2(a)^1(b)^0(a)^1$	−0.383
$S_2(^1A)$	38 814	$(a)^2(b)^2(a)^2(b)^2(a)^1(b)^1(a)^0$	0.686
		$(a)^2(b)^2(a)^2(b)^1(a)^2(b)^0(a)^1$	−0.317

[a] Electron configurations whose CI (configuration interaction) coefficients are larger than 0.30.

To estimate the magnitude of SOC in the target compounds, SOCI wave functions are constructed using the MCSCF orbitals. Unfortunately, the external space could include only 30 orbitals, which have the lowest eigenvalues of the standard MCSCF Fock operator, due to computer-resource limitations. The SOC matrices include both the singlet and triplet states listed in Table 1, and their matrix elements are computed within the Z_{eff} approximation.[35−40] All calculations were carried out using the GAMESS suite of program codes.[53]

3. Results and Discussion

3.1. Characterization of Low-Lying Excited States. The geometrical structures of bis-[2-(2-thienyl)-pyridine] platinum-(II) ($Pt(thpy)_2$) and the corresponding palladium(II) complex ($Pd(thpy)_2$) were optimized at the B3LYP/SBKJC+p level of theory. Since it has been experimentally demonstrated that these complexes, as well as their analogous metal complexes, have N,N-cis structures,[18,21,24,54] the cis isomers of the target complexes were employed in the present investigation. In fact, the cis isomers are calculated to be more stable than the corresponding trans isomers by 8.1 kcal/mol at the B3LYP/SBKJC+p level of theory. The optimized geometries of their ground states have C_2 symmetry, and the angles between the N_6-C_2 bond and the $C_2-Pt_3-C_4/C_2-Pd_3-C_4$ plane are 10−12° (see Figure 1). These cis and trans geometries are confirmed to be energy minima by achieving vibrational frequency analyses.

Since the process of phosphorescence is the target of the present investigation, the optimized geometries are also obtained for the lowest triplet in both the Pd and Pt cis complexes. The angles between the N_6-C_2 bond and the $C_2-Pt_3-C_4$ plane are almost unchanged (11.7° (Pd) and 10.3° (Pt)). The energy differences between the C_{2v} and C_2 symmetric structures are calculated to be 2.1 (Pd) and 3.9 (Pt) kcal/mol on the lowest triplet potential energy surfaces at the MCSCF+SOCI/SBKJC+p

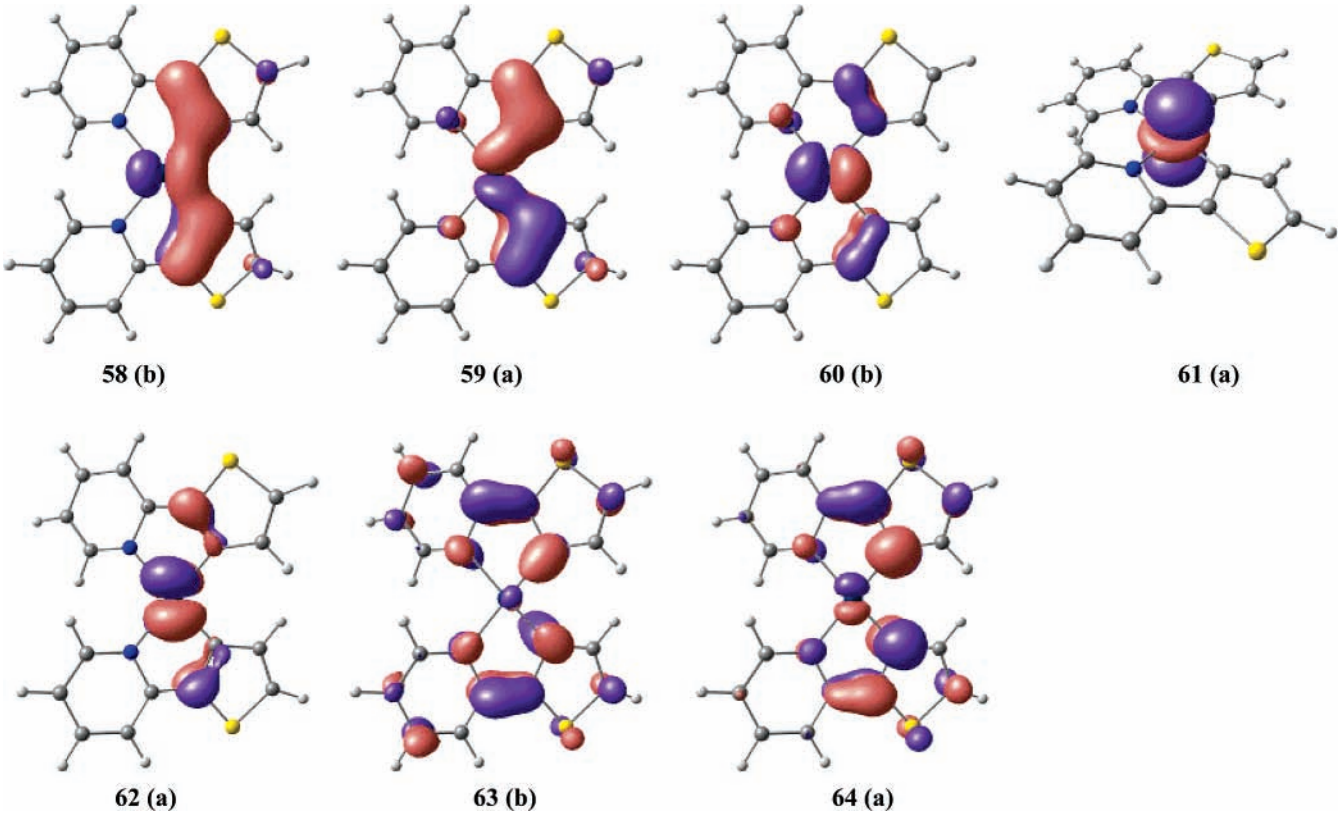

Figure 2. MCSCF natural orbitals obtained for $Pt(thpy)_2$.

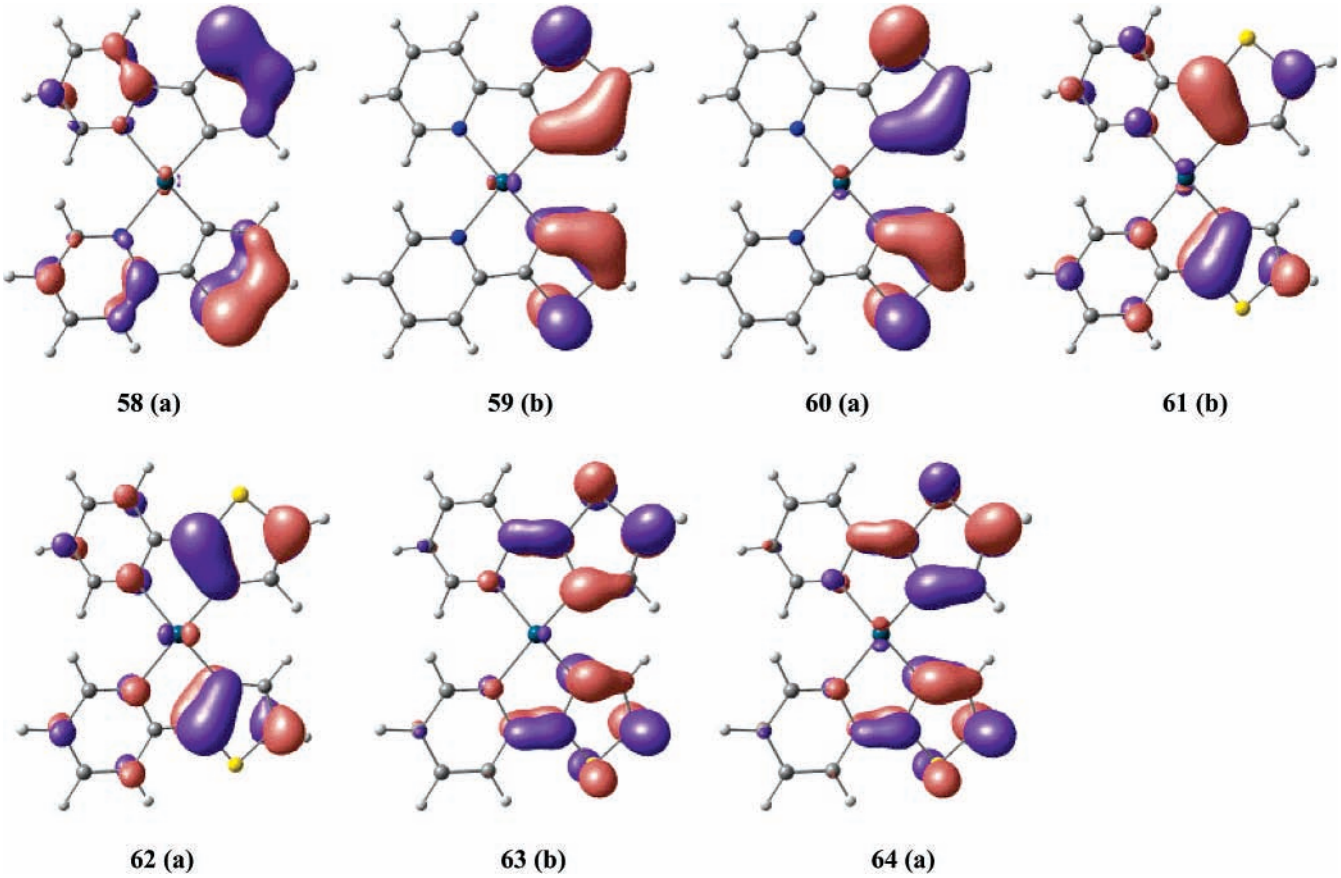

Figure 3. MCSCF natural orbitals obtained for $Pd(thpy)_2$.

level of theory. Note that the energy differences in the ground states are provided as 1.9 (Pd) and 0.4 (Pt) kcal/mol at the optimized geometries for the triplets, respectively.[55]

Table 1 lists the relative energies of several low-lying states at the C_2 cis geometries optimized for the lowest triplet obtained using the MCSCF(10,7)+SOCI method. In $Pt(thpy)_2$, the lowest

TABLE 2: Spin−Orbit Coupling Constants [cm^{-1}] between Low-Lying Singlet and Triplet States in Pt(thpy)$_2$

$\langle S_0(^1A)\|H_{SO}\|T_1(^3A)\rangle = 179$	$\langle S_0(^1A)\|H_{SO}\|T_2(^3B)\rangle = 339$	$\langle S_0(^1A)\|H_{SO}\|T_3(^3B)\rangle = 160$
$\langle S_1(^1A)\|H_{SO}\|T_1(^3A)\rangle = 0$	$\langle S_1(^1A)\|H_{SO}\|T_2(^3B)\rangle = 2280$	$\langle S_1(^1A)\|H_{SO}\|T_3(^3B)\rangle = 2255$
$\langle S_2(^1B)\|H_{SO}\|T_1(^3A)\rangle = 2527$	$\langle S_2(^1B)\|H_{SO}\|T_2(^3B)\rangle = 1228$	$\langle S_2(^1B)\|H_{SO}\|T_3(^3B)\rangle = 1877$
$\langle S_3(^1B)\|H_{SO}\|T_1(^3A)\rangle = 1344$	$\langle S_3(^1B)\|H_{SO}\|T_2(^3B)\rangle = 2214$	$\langle S_3(^1B)\|H_{SO}\|T_3(^3B)\rangle = 1765$

three triplet states [T_1 (^{3}A), T_2 (^{3}B), and T_3 (^{3}B)] are in the energy range of only 2747 cm^{-1}, and the corresponding singlet states [S_1 (^{1}A), S_2 (^{1}B), and S_3 (^{1}B)] are higher than these states by 3050−4370 cm^{-1}. These states mainly have the MLCT character (see Figure 2), which is consistent with the experimental reports.[26,49,52] Pierloot et al.[34] reported that the low-lying excited singlet states have MLCT character, when the geometrical structure is assumed to have C_{2v} geometry, at the CASPT2 level of theory. They also reported that the lowest triplet state has LC character, but the experimental study indicates that the triplet should have MLCT character. The present study agrees with the experimental results, even though C_2 geometry is used and the emission energies to the ground state are underestimated by about 3000 cm^{-1}. The *0−0 transition energy* from the lowest triplet state to the ground state is observed to be 17 156 cm^{-1} by Wiedenhofer et al.[52] In the present study, the *0−0 transition energy* (not shown in Table 1) is estimated to be 19 248 cm^{-1} at the MCSCF+SOCI/SBKJC+p level of theory and to be 17 533 cm^{-1} after the inclusion of the SOC effects. This result indicates that it is greatly important to include the SOC effects in the study of such complexes.

On the contrary, the singlet−triplet energy gaps in Pd(thpy)$_2$ are relatively larger than those in Pt(thpy)$_2$. Even though the Pd's d orbitals were initially chosen as the occupied active orbitals, very small coefficients were obtained for the d orbitals after the MCSCF iterations and, as a result, all active orbitals have large components of the ligands' π orbitals as shown in Figure 3. Therefore, in Pd(thpy)$_2$ the low-lying triplet excited states should be recognized as LC ($\pi - \pi^*$). This result is supported by Pierloot et al., as well as several experimental results[48−50] on the basis of highly resolved excitation and emission spectra in Shpol'skii matrices.

Yersin et al.[49] observed the 0−0 peak at the energy of 18 418 cm^{-1}, while the *0−0 transition energy* between the ground state and the lowest excited triplet state is estimated to be 22 038 cm^{-1} within the relativistic scheme in the present study. The present method overestimates the transition energy by about 3500 cm^{-1}. It may be necessary to perform more sophisticated calculations for this complex in the near future.

3.2. Spin−Orbit Coupling between Triplets and Singlets. The emission from the lowest triplet state to the ground state, so-called phosphorescence, is a spin-forbidden process. To describe such spin-forbidden processes, the SOC effects need to be considered. Tables 2 and 4 summarize the SOC constants between low-lying singlets and triplets calculated using the Z_{eff} approximation,[35−40] and Tables 3 and 5 list the emission energies from low-lying spin-mixed states to the ground state and the corresponding transition dipole moments (TDMs). The SOCs between the adiabatic ground state (S_0) and three low-lying adiabatic triplet states (T_1, T_2, and T_3) in Pt(thpy)$_2$ are about 160−339 cm^{-1} and are apparently smaller than those among the excited singlets and triplets (see Table 2). These results suggest that, in a relativistic picture, the low-lying excited spin-mixed states have large coefficients of both low-lying excited singlets and triplets in this Pt complex. As a result, TDMs between the lowest spin-mixed state (namely the ground state in the relativistic picture) and some low-lying excited spin-mixed states are large as listed in Table 3 (see the next section).

TABLE 3: Energy Differences ΔE [cm^{-1}] and Transition Dipole Moments (TDMs) [eÅ] between the Lowest Spin-Mixed State (SM0) and Low-Lying Spin-Mixed States in Pt(thpy)$_2$

	ΔE	TDM	character		
SM0	0		S_0 ^{1}A[A][a]	1.00[b]	$\alpha\beta-\beta\alpha$[c]
SM1	17 231	0.0007	T_1 ^{3}A[A]	0.61	$\alpha\beta+\beta\alpha$
			T_2 ^{3}B[B]	0.25	$\alpha\alpha+\beta\beta$
			T_3 ^{3}B[B]	0.13	$\alpha\alpha+\beta\beta$
SM2	17 252	0.0940	S_3 ^{1}B[A]	0.01	$\alpha\beta-\beta\alpha$
			T_1 ^{3}A[B]	0.64	$\alpha\alpha+\beta\beta$
			T_2 ^{3}B[A]	0.24	$\alpha\beta+\beta\alpha$
			T_3 ^{3}B[A]	0.12	$\alpha\alpha+\beta\beta$
SM3	17 934	0.1335	S_2 ^{1}B[A]	0.14	$\alpha\beta-\beta\alpha$
			T_1 ^{3}A[B]	0.85	$\alpha\alpha-\beta\beta$
SM4	18 156	0.0853	S_1 ^{1}A[A]	0.22	$\alpha\beta-\beta\alpha$
			T_2 ^{3}B[B]	0.52	$\alpha\alpha-\beta\beta$
			T_3 ^{3}B[B]	0.25	$\alpha\alpha-\beta\beta$
SM5	19 491	0.0039	T_1 ^{3}A[A]	0.21	$\alpha\beta+\beta\alpha$
			T_2 ^{3}B[B]	0.42	$\alpha\alpha+\beta\beta$
			T_3 ^{3}B[B]	0.37	$\alpha\alpha-\beta\beta$
SM6	19 948	0.1952	S_2 ^{1}B[A]	0.14	$\alpha\beta-\beta\alpha$
			T_2 ^{3}B[A]	0.50	$\alpha\beta+\beta\alpha$
			T_3 ^{3}B[A]	0.27	$\alpha\beta+\beta\alpha$
SM7	20 371	0.1067	S_1 ^{1}A[A]	0.38	$\alpha\beta-\beta\alpha$
			T_2 ^{3}B[B]	0.22	$\alpha\alpha+\beta\beta$
			T_3 ^{3}B[B]	0.39	$\alpha\alpha+\beta\beta$
SM8	21 050	0.6652	S_3 ^{1}B[A]	0.23	$\alpha\beta-\beta\alpha$
			T_1 ^{3}A[B]	0.25	$\alpha\alpha+\beta\beta$
			T_2 ^{3}B[A]	0.10	$\alpha\beta+\beta\alpha$
			T_3 ^{3}B[A]	0.37	$\alpha\beta+\beta\alpha$
SM9	24 636	0.0004	T_1 ^{3}A[A]	0.18	$\alpha\beta+\beta\alpha$
			T_2 ^{3}B[B]	0.33	$\alpha\alpha+\beta\beta$
			T_3 ^{3}B[B]	0.50	$\alpha\alpha+\beta\beta$
SM10	25 886	0.1071	S_1 ^{1}A[A]	0.40	$\alpha\beta-\beta\alpha$
			T_2 ^{3}B[B]	0.25	$\alpha\alpha-\beta\beta$
			T_3 ^{3}B[B]	0.35	$\alpha\alpha-\beta\beta$
SM11	26 252	0.2944	S_2 ^{1}B[A]	0.67	$\alpha\beta-\beta\alpha$
			T_1 ^{1}A[B]	0.12	$\alpha\alpha-\beta\beta$
			T_3 ^{3}B[A]	0.13	$\alpha\beta+\beta\alpha$
SM12	28 002	1.1299	S_3 ^{1}B[A]	0.73	$\alpha\beta-\beta\alpha$
			T_3 ^{3}B[A]	0.11	$\alpha\beta+\beta\alpha$

[a] Adiabatic components. [b] Weights of adiabatic states. [c] Spin functions

Therefore, strong emission is expected to be observed in this complex. Since the excited spin-mixed states have large components of the adiabatic triplet states, the emission can be recognized as "*phosphorescence*". In the following section, the transition probabilities from these excited spin-mixed states will be estimated.

The SOCs in Pd(thpy)$_2$ are apparently smaller than those in Pt(thpy)$_2$ as listed in Table 4. This is mainly because the low-lying spin-mixed states are LC states; in other words, the SOCs are observed only on the ligands and are rather small because the ligands do not consist of any heavy metal elements. In addition, the TDMs are also small between the lowest spin-mixed state and the low-lying excited spin-mixed states (see Table 5). Accordingly, it can be concluded that, at room temperature, no strong phosphorescence should be observed in the Pd complex. In fact, phosphorescence in Pd(thpy)$_2$ has been observed only at cryogenic temperatures.[22,47,49,56] This experimental result strongly supports the present results, since nonradiative transitions would be suppressed under such experimental conditions.

TABLE 4: Spin−Orbit Coupling Constants [cm^{-1}] between Low-Lying Singlet and Triplet States in Pd(thpy)$_2$

$\langle S_0(^1A)\|H_{SO}\|T_1(^3B)\rangle = 4$	$\langle S_0(^1A)\|H_{SO}\|T_2(^3A)\rangle = 2$	$\langle S_0(^1A)\|H_{SO}\|T_3(^3B)\rangle = 6$
$\langle S_1(^1B)\|H_{SO}\|T_1(^3B)\rangle = 1$	$\langle S_1(^1B)\|H_{SO}\|T_2(^3A)\rangle = 5$	$\langle S_1(^1B)\|H_{SO}\|T_3(^3B)\rangle = 1$
$\langle S_2(^1A)\|H_{SO}\|T_1(^3B)\rangle = 10$	$\langle S_2(^1A)\|H_{SO}\|T_2(^3A)\rangle = 1$	$\langle S_2(^1A)\|H_{SO}\|T_3(^3B)\rangle = 9$

TABLE 5: Energy Differences ΔE [cm^{-1}] and Transition Dipole Moments (TDMs) [e Å] between the Lowest Spin-Mixed State (SM0) and Low-Lying Spin-Mixed States in Pd(thpy)$_2$

	ΔE	TDM	character		
SM0 (A)	0		S_0 ^{1}A[A]^a	1.00^b	$\alpha\beta-\beta\alpha^c$
SM1 (A)	22 137	0.0000	T_1 ^{3}B[A]	0.95	$\alpha\beta+\beta\alpha$
SM2 (B)	22 137	0.0002	T_1 ^{3}B[B]	0.95	$\alpha\alpha-\beta\beta$
SM3 (B)	22 138	0.0010	T_1 ^{3}B[B]	1.00	$\alpha\alpha+\beta\beta$
SM4 (B)	22 153	0.0002	T_2 ^{3}A[B]	1.00	$\alpha\alpha+\beta\beta$
SM5 (A)	22 154	0.0001	T_2 ^{3}A[A]	0.95	$\alpha\beta+\beta\alpha$
SM6 (B)	22 154	0.0000	T_2 ^{3}A[B]	0.95	$\alpha\alpha-\beta\beta$
SM7 (B)	34 025	0.0009	T_3 ^{3}B[B]	0.99	$\alpha\alpha-\beta\beta$
SM8 (A)	34 025	0.0001	T_3 ^{3}B[A]	0.99	$\alpha\beta+\beta\alpha$
SM9 (B)	34 025	0.0030	T_3 ^{3}B[B]	1.00	$\alpha\alpha+\beta\beta$
SM10 (B)	34 232	0.0003	T_4 ^{3}A[B]	1.00	$\alpha\alpha+\beta\beta$
SM11 (B)	34 232	0.0005	T_4 ^{3}A[B]	0.99	$\alpha\alpha-\beta\beta$
SM12 (A)	34 232	0.0000	T_4 ^{3}A[A]	0.99	$\alpha\beta+\beta\alpha$
SM13 (A)	37 184	0.4963	S_1 ^{1}B[A]	1.00	$\alpha\beta-\beta\alpha$
SM14 (A)	38 814	1.5937	S_2 ^{1}A[A]	1.00	$\alpha\beta-\beta\alpha$

^{a} Adiabatic components. ^{b} Weights of adiabatic states. ^{c} Spin functions

3.3. Transition Probability among Spin-Mixed States. Let us first define the wave function of the *n*th vibrational state in the *i*th spin-mixed state as $|\Psi_i^n\rangle = |\Phi_i\rangle|\chi_n^i\rangle$, where $|\Phi_i\rangle$ represents the wave function of the *i*th spin-mixed state and its *n*th vibrational state has the wave function $|\chi_n^i\rangle$. In the relativistic picture, the wave function $|\Phi_i\rangle$ of a low-lying spin-mixed state is expressed by the mixture of the adiabatic states:

$$|\Phi_i\rangle = \sum_k c_k|S_k\rangle + \sum_l c_l|T_l\rangle$$

since states of higher spin multiplicity are too high in energy to be mixed remarkably into $|\Phi_i\rangle$. For the emission from a low-lying spin-mixed state $|\Psi_i^n\rangle$ to the lowest spin-mixed state $|\Psi_0^m\rangle$ (the ground state), the transition probability of the emission can be provided by Fermi's golden rule as follows:

$$P_{i0} = \frac{2\pi}{\hbar}|\langle\Psi_i^n|H'|\Psi_0^m\rangle|^2\rho(\Psi_0^m) = \frac{2\pi}{\hbar}|(\chi_n^i|\langle\Phi_i|H'|\Phi_0\rangle|\chi_m^0)|^2\rho(\Psi_0^m)$$

where $\hbar$ is Planck's constant and $\rho(\Psi_0^m)$ is the density of vibrational, rotational, and translational states in the ground state. Within dipole approximation, $H' = \mu = $ er, and then

$$P_{i0} = \frac{2\pi}{\hbar}|(\chi_n^i|\langle\Phi_i|\mu|\Phi_0\rangle|\chi_m^0)|^2\rho(\Psi_0^m)$$

In most stable molecular systems, $|\Phi_0\rangle$ has a large component of the adiabatic ground state S_0. Meanwhile, $|\Phi_i\rangle$ is provided by a relatively strong mixture of singlets and triplets in the relativistic picture, so that $\langle\Phi_i|\mu|\Phi_0\rangle$ can be nonzero when their symmetry is satisfied even though $\langle T_l|\mu|S_k\rangle = 0$. In the present investigation, the emission is recognized as fluorescence when $|\Phi_i\rangle$ mainly has singlet components, while it is as recognized as phosphorescence when $|\Phi_i\rangle$ mainly has triplet components. Because the state density $\rho(\Psi_0^m)$ is the same for the both processes, the emission probability can be discussed on the basis of the following interaction integrals:

$$I_{nm}^{i0} = (\chi_n^i|\langle\Phi_i|\mu|\Phi_0\rangle|\chi_m^0)$$

The vibrational wave functions, $|\chi_n^i\rangle$ and $|\chi_m^0\rangle$, can be provided as the product of vibrational wave functions corresponding to various kinds of normal modes. However, it is troublesome to explicitly treat all vibrational modes in both electronic states. The present investigation focused on the twisting motion of the ligands, because the most stable cis structures have C_2 symmetry in the ground states of Pt(thpy)$_2$ and Pd (thpy)$_2$), and the corresponding C_{2v} structures are the transition states for their optical isomerization reactions. The energy barriers for these isomerizations are calculated to be only 3−4 kcal/mol at the MCSCF+SOCI/SBKJC+p level of theory. All the other vibrational modes were assumed to have the same harmonic functions in both the initial and final states.

Because of the small energy barriers, the linear synchronous transits (LST) between the C_2 and C_{2v} structures were chosen as the reaction coordinate (corresponding to the vibrational coordinate of the ligands' twist motion). As mentioned in the previous section, because the present study focuses on phosphorescence, the optimized geometry for the lowest triplet was used at the energy minima and the transition states in these molecular systems. When the center-of-mass is fixed at the origin of the Cartesian coordinates and the principal axes of molecular rotation are maintained as those of the Cartesian coordinates, the root-mean-square (RMS) of the displacement from the transition state geometry (C_{2v}) is taken as the horizontal axis in Figure 4. Then, the energy minimum of the lowest triplet appears at the RMS of ±0.48 in the Pt complex. Along this LST, the energy curves of low-lying spin-mixed states and the integrals $\langle\Phi_i|\mu|\Phi_0\rangle$ were calculated as a function of the displacement. By using these potential energy curves, the vibrational wave functions $|\chi_n^i\rangle$ and $|\chi_m^0\rangle$ of the ligand twisting mode and the corresponding vibrational energies were obtained using the discrete variable representation (DVR) method.[57] Note that the energy barrier in the ground state becomes rather small (0.4 kcal/mol) along this reaction coordinate, as illustrated in Figure 4. This is of course because the optimized geometries for the lowest triplet are used.

Figure 4 plots the potential energy curves of the lowest 13 spin-mixed states along the LST. For simplicity, the spin-mixed states are named by their energetic order at the energy minimum of the adiabatic S_0 state, such as SM0, SM1, SM2, and so on. As mentioned in the previous section, the lowest spin-mixed state SM0 consists of the adiabatic ground state S_0(^{1}A[A]) with the weight of 99%, where the spin function $(1/\sqrt{2})\{\alpha\beta - \beta\alpha\}$ belongs to the A representation of C_2 symmetry indicated by [A]. The lowest excited state SM1 has T_1(^{3}A[A]) as a main configuration, where the spin function $(1/\sqrt{2})\{\alpha\beta + \beta\alpha\}$ also belongs to the A representation of C_2 symmetry. Since this state does not have a large singlet component, the TDM is very small, and as a result, the transition probability I_{0m}^{10} is considerably small (see Table 6). The second lowest state SM2 also has T_1-(^{3}A[B]), where its spin function is $(1/\sqrt{2})\{\alpha\alpha + \beta\beta\}$, and is only 21 cm^{-1} higher than SM1 at the energy minimum of SM2. The TDM between SM0 and SM2 is larger than that between

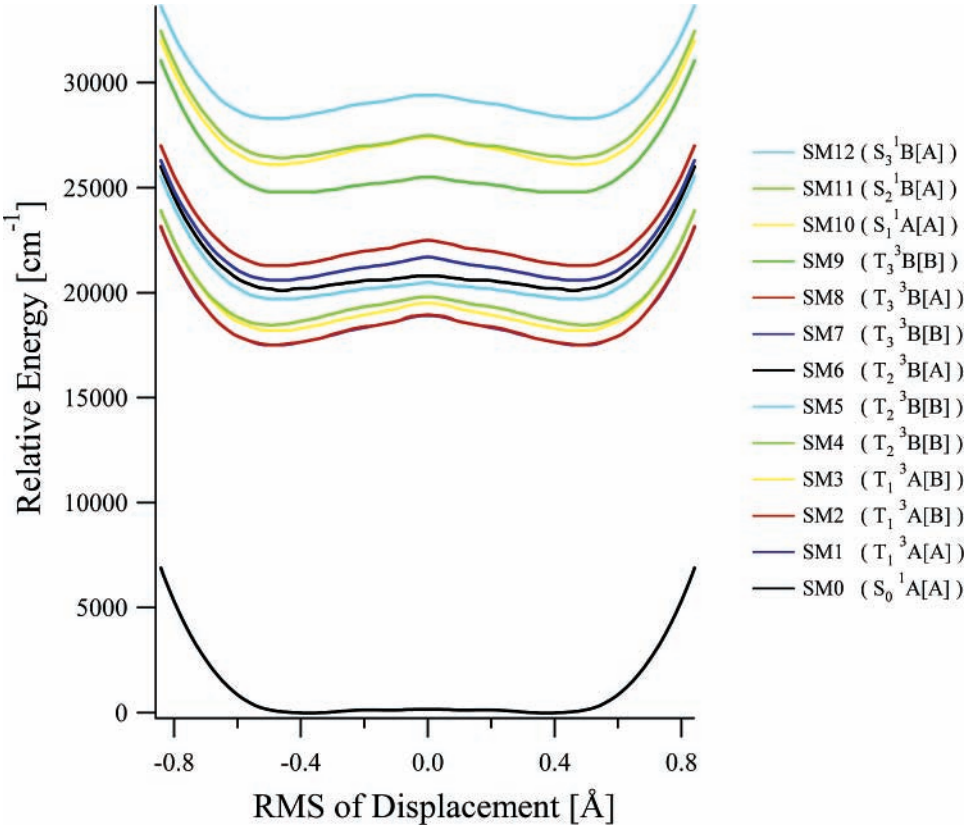

Figure 4. Potential energy curves for 13 low-lying spin-mixed states in Pt(thpy)$_2$ obtained at the MCSCF+SOCI/SBKJC+p level of theory. The main adiabatic component in each spin-mixed state is shown in parentheses (see Table 3).

TABLE 6: Interaction Integrals I_{nm}^{if} [e Å] and Energy Differences $\Delta E_{nm}^{if} = E_n^i - E_m^f$ [cm^{-1}] of Low-Lying Vibrational States in Pt(thpy)$_2$[a]

m	I_{0m}^{10}	ΔE_{0m}^{10}	I_{0m}^{20}	ΔE_{0m}^{20}	I_{0m}^{30}	ΔE_{0m}^{30}	I_{0m}^{40}	ΔE_{0m}^{40}
0	0.0001	17 533	0.0260	17 554	0.0455	18 217	0.0003	18 486
1	0.0000	17 533	0.0004	17 554	0.0006	18 217	0.0195	18 486
2	0.0001	17 482	0.0308	17 503	0.0496	18 166	0.0245	18 435
3	0.0001	17 482	0.0301	17 503	0.0486	18 166	0.0251	18 435
4	0.0001	17 433	0.0311	17 454	0.0465	18 117	0.0273	18 386
5	0.0001	17 433	0.0311	17 454	0.0465	18 117	0.0273	18 386
6	0.0001	17 406	0.0140	17 427	0.0201	18 090	0.0128	18 359
7	0.0001	17 404	0.0159	17 425	0.0228	18 088	0.0146	18 357
8	0.0001	17 388	0.0217	17 409	0.0303	18 072	0.0205	18 341
9	0.0001	17 384	0.0233	17 405	0.0324	18 068	0.0221	18 337
10	0.0001	17 365	0.0187	17 386	0.0253	18 049	0.0183	18 318

m	I_{0m}^{50}	ΔE_{0m}^{50}	I_{0m}^{60}	ΔE_{0m}^{60}	I_{0m}^{70}	ΔE_{0m}^{70}	I_{0m}^{80}	ΔE_{0m}^{80}
0	0.0016	19 723	0.0983	20 167	0.0007	20 631	0.0035	21 315
1	0.0000	19 723	0.0013	20 167	0.0492	20 631	0.2559	21 315
2	0.0014	19 672	0.0769	20 116	0.0453	20 580	0.2556	21 264
3	0.0014	19 672	0.0754	20 116	0.0463	20 580	0.2608	21 264
4	0.0011	19 623	0.0544	20 067	0.0381	20 531	0.2290	21 215
5	0.0011	19 623	0.0544	20 067	0.0381	20 531	0.2291	21 215
6	0.0004	19 596	0.0203	20 040	0.0154	20 504	0.0954	21 188
7	0.0005	19 594	0.0228	20 038	0.0174	20 502	0.1079	21 186
8	0.0006	19 578	0.0280	20 022	0.0223	20 486	0.1405	21 170
9	0.0007	19 574	0.0292	20 018	0.0235	20 482	0.1492	21 166
10	0.0005	19 555	0.0209	19 999	0.0176	20 463	0.1136	21 147

[a] For example, I_{0m}^{10} and ΔE_{0m}^{10} are the interaction integral and the energy difference between the 0th vibrational state in SM1 and the mth vibrational state in SM0.

SM0 and SM1 because SM2 has a small component of S_3(^{1}B[A]) and the adiabatic TDM (1.4 [e Å]) between S_0(^{1}A[A]) and S_3(^{1}B[A]) is remarkably larger than the others. As a result, I_{0m}^{20} is larger than I_{0m}^{10}, as listed in Table 6. As mentioned above, SM1 and SM2 should be recognized as the sublevels of T_1, while the third sublevel of T_1 appears as SM3. SM4, SM5, and SM6 are the sublevels of T_2(^{3}B[B]), and SM7, SM8, and SM9 are the sublevels of T_3(^{3}B[A]). SM8 has a large TDM to the ground state SM0, but it may be natural that the nonradiative transition from these states to lower excited spin-mixed states would be very fast because the state is high in energy, so that the emission from these states would not be observed. Thus, the present investigation suggests that the emission from SM2 would be observed rather than from SM1, and the main peak of the emission would appear at the energy of 17 554 cm^{-1} (*0−0 transition energy* corresponding to the intensity I_{00}^{20}). In addition, because SM2 has large adiabatic triplet components, this emission should be recognized as "*phosphorescence*".

SM10, SM11, and SM12 have adiabatic S_1(^{1}A[A]), S_2(^{1}B[A]), and S_3(^{1}B[A]) components as a main configuration, respectively. These states have large TDMs to the ground state, but fast nonradiative relaxation (or ISC) is expected to occur from these states to low-lying *excited* states (the Kasha rule) and, as a result, no emission would be observed from these states.

The present conclusion is supported by several experiments: A strong emission was observed at $\lambda_{max} = 580$ nm ($\approx$17 200 cm^{-1}) in both the photoluminescence (PL)[18−20,30] and electroluminescence (EL)[16,28,33] spectra of Pt(thpy)$_2$. Yersin et al. also reported that the transition between the lowest triplet sublevel and the ground state is forbidden, and that the radiative transition from the next low-lying triplet sublevel is faster, when it was dissolved in Shpol'skii matrix.[26,27]

The same investigation has been performed for Pd(thpy)$_2$. The integrals I_{0m}^{i0} ($i = 1-12$) are found to be smaller than 2.9 $\times$ 10^{-3} [e Å] (see Table 1S in the Supporting Information). Accordingly, it should be considered that fast ISC occurs from

low-lying excited spin-mixed states to the lowest spin-mixed state (ground state) and no strong phosphorescence is observed in the Pd complex at room temperature, as reported experimentally.[22] Thus, the present investigation confirms that this molecule is inappropriate for use as phosphorescent OLEDs.

4. Summary

The radiative and nonradiative processes from the excited states in the platinum and palladium complexes were investigated within the relativistic picture, where SOC effects are explicitly considered. The transition probabilities among the low-lying spin-mixed states in these complexes are estimated using the DVR method based on the assumption that the system obeys Fermi's golden rule. The calculated results indicate that $Pt(thpy)_2$ has strong SOCs among excited singlets and triplets and that, as a result, a fast nonradiative transition occurs to the low-lying excited spin-mixed states. Then, the radiative transition occurs from these low-lying excited spin-mixed states to the lowest spin-mixed state (the ground state); that is to say, phosphorescence should be observed in $Pt(thpy)_2$. On the other hand, since weak SOC effects are obtained in $Pd(thpy)_2$, no phosphorescence is expected to be observed at room temperature. These results are in good agreement with the experimental reports.

This investigation would be the first application of the relativistic method[35−40] to large-sized molecules in the OLED fields of industrial production. We are now investigating the transition probabilities of phosphorescence in various transition metal compounds in order to understand emission mechanisms in OLED compounds and to design better OLED compounds for industrial production. It is generally considered that one singlet and three triplet excitons are roughly generated by electric excitation in the OLEDs,[58] since a triplet has three spin sublevels. Under this assumption, the internal quantum efficiency (η_{int}) in fluorescent OLEDs is limited to be at most 25% and η_{int} could be 75% for phosphorescent OLEDs. If fast ISC occurred, or if a singlet exciton was converted quickly into a triplet such as the Pt complex, η_{int} for phosphorescent OLEDs could reach 100%. In fact, very high efficiency ($\eta_{int} \sim 100\%$) has been reported, when platinum and iridium complexes are employed as dyes in the phosphorescent OLEDs.[1,3−5,8,9] In addition, the energy of phosphorescence (namely, emission color) is also important for high-performance full-color display. Right now, most of the current OLED materials provide low-energy emission, and it is eagerly expected to propose new OLEDs of high-energy phosphorescence, or blue-color OLED materials. Since the present investigation succeeded in theoretically explaining the experimental results for $Pd(thpy)_2$ and $Pt(thpy)_2$, our results on various kinds of transition metal compounds within the relativistic picture would become very useful in order to understand emission mechanisms in OLED compounds and to design better OLED compounds. Our forthcoming papers[59] will further explore these topics.

Acknowledgment. The authors thank Prof. Shimakura in Niigata University for his useful suggestions and comments.

Supporting Information Available: Table 1S listing the interaction integrals I_{nm}^{if} and the corresponding energy differences $\Delta E_{nm}^{if} = E_n^i - E_m^f$ of low-lying vibrational states in $Pd(thpy)_2$. This material is available free of charge via the Internet at http://pubs.acs.org.

References and Notes

(1) Baldo, M. A.; O'Brien, D. F.; You, Y.; Shoustikov, A.; Sibley, S.; Thompson, M. E.; Forrest, S. R. *Nature (London)* **1998**, *151*, 395.
(2) O'Brien, D. F.; Baldo, M. A.; Thompson, M. E.; Forrest, S. R. *Appl. Phys. Lett.* **1999**, *74*, 442.
(3) Baldo, M. A.; Lamansky, S.; Burrows, P. E.; Thompson, M. E.; Forrest, S. R. *Appl. Phys. Lett.* **1999**, *75*, 4.
(4) Adachi, C.; Baldo, M. A.; Forrest, S. R. *Appl. Phys. Lett.* **2000**, *77*, 904.
(5) Adachi, C.; Baldo, M. A.; Forrest, S. R.; Lamansky, S.; Thompson, M. E.; Kwong, R. C. *Appl. Phys. Lett.* **2001**, *78*, 1622.
(6) Adachi, C.; Kwong, R. C.; Djurovich, P.; Adamovich, V.; Baldo, M. A.; Thompson, M. E.; Forrest, S. R. *Appl. Phys. Lett.* **2001**, *79*, 2082.
(7) Wang, Y.; Herron, N.; Grushin, V. V.; LeCloux, D. D.; Petrov, V. A. *Appl. Phys. Lett.* **2001**, *79*, 449.
(8) Adachi, C.; Baldo, M. A.; Thompson, M. E.; Forrest, S. R. *Bull. Am. Phys. Soc.* **2001**, *46*, 863.
(9) Adachi, C.; Baldo, M. A.; Thompson, M. E.; Forrest, S. R. *J. Appl. Phys.* **2001**, *90*, 5048.
(10) Grushin, V. V.; Herron, N.; LeCloux, D. D.; Marshall, W. J.; Petrov, V. A.; Wang, Y. *Chem. Commun.* **2001**, 1494.
(11) Ostrowski, J. C.; Robinson, M. R.; Heeger, A. J.; Bazan, C. C. *Chem. Commun.* **2002**, 784.
(12) Cheng, G.; Li, F.; Duan, Y.; Feng, J.; Liu, S.; Qiu, S.; Lin, D.; Ma, Y.; Lee, S. T. *Appl. Phys. Lett.* **2003**, *82*, 4224.
(13) Tokito, S.; Iijima, T.; Tsuzuki, T.; Sato, F. *Appl. Phys. Lett.* **2003**, *83*, 2459.
(14) Holmes, R. J.; D'Andrade, M. W.; Forrest, S. R.; Ren, X.; Li, J.; Thompson, M. E. *Appl. Phys. Lett.* **2003**, *83*, 3818.
(15) Lamansky, S.; Djurovich, P.; Murphy, D.; Abdel-Razzaq, F.; Lee, H.-E.; Adachi, C.; Burrows, P. E.; Forrest, S. R.; Thompson, M. E. *J. Am. Chem. Soc.* **2001**, *123*, 4304.
(16) Cocchi, M.; Fattori, V.; Virgili, D.; Sabatini, C.; Marco, P. Di.; Maestri, M.; Kalinowski, J. *Appl. Phys. Lett.* **2004**, *84*, 1052.
(17) Klessinger, M. M. J. *Excited States and Photochemistry of Organic Molecules*; VCH Publishers: New York, 1995.
(18) Chassot, L.; Müller, E.; von Zelewsky, A. *Inorg. Chem.* **1984**, *23*, 4249.
(19) Bonafede, S.; Ciano, M.; Bolletta, F.; Balzani, V.; Chassot, L.; von Zelewsky, A. *J. Phys. Chem.* **1986**, *90*, 3836.
(20) Sandrini, D.; Maestri, M.; Balzani, V.; Chassot, L.; von Zelewsky, A. *J. Am. Chem. Soc.* **1987**, *109*, 7720.
(21) Chassot, L.; von Zelewsky, A. *Inorg. Chem.* **1987**, *26*, 2814.
(22) Barigelletti, F.; Sandrini, D.; Maestri, M.; Balzani, V.; von Zelewsky, A.; Chassot, L.; Jolliet, P.; Maeder, U. *Inorg. Chem.* **1988**, *27*, 3644.
(23) Cummings, S. D.; Eisenberg, R. *J. Am. Chem. Soc.* **1996**, *118*, 1949.
(24) Jolliet, P.; Gianini, M.; von Zelewsky, A.; Bernardinelli, G.; Stoeckly-Evans, H. *Inorg. Chem.* **1996**, *35*, 4883.
(25) Büchner, R.; Field, J. S.; Haines, R. J.; Cunningham, C. T.; McMillin, D. R. *Inorg. Chem.* **1997**, *36*, 3952.
(26) Schmidt, J.; Strasser, J.; Yersin, H. *Inorg. Chem.* **1997**, *36*, 3957.
(27) Strasser, J.; Donges, D.; Humbs, W.; Kulikova, M. V.; Balashev, K. P.; Yersin, H. *J. Lumin.* **1998**, *76−77*, 611.
(28) Lamansky, S.; Kwong, R. C.; Nugent, M.; Djurovich, P. I.; Thompson, M. E. *Org. Electron.* **2001**, *2*, 53.
(29) Lu, W.; Mi, B.-X.; Chan, M. C. W.; Hui, Z.; Zhu, N.; Lee, S.-T.; Che, C.-M. *Chem. Commun.* **2002**, 206.
(30) Brooks, J.; Babayan, Y.; Lamansky, S.; Djurovich, P. I.; Tsybam, I.; Bau, R.; Thompson, M. E. *Inorg. Chem.* **2002**, *41*, 3055.
(31) Lin, Y.-Y.; Chan, S.-C.; Chan, M. C. W.; Hou, Y.-J.; Zhu, N.; Che, C.-M.; Liu, Y.; Wang, Y. *Chem.—Eur. J.* **2003**, *9*, 1264.
(32) Lu, W.; Chan, M. C. W.; Cheung, K.-K.; Che, C.-M. *Organometallics* **2001**, *20*, 2477.
(33) Shoustikov, A. A.; You, Y.; Thompson, M. E. *IEEE J. Sel. Top. Quantum Electron.* **1998**, *4*, 3.
(34) Pierloot, K.; Ceulemans, A.; Merchán, M.; Serrano-Andrés, L. *J. Phys. Chem. A* **2000**, *104*, 4374.
(35) Koseki, S.; Schmidt, M. W.; Gordon, M. S. *J. Phys. Chem.* **1992**, *96*, 10768.
(36) Koseki, S.; Gordon, M. S.; Schmidt, M. W.; Matsunaga, N. *J. Phys. Chem.* **1995**, *99*, 12764.
(37) Koseki, S.; Schmidt, M. W.; Gordon, M. S. *J. Phys. Chem.* **1998**, *102*, 10430.
(38) Koseki, S.; Fedorov, D. G.; Schmidt, M. W.; Gordon, M. S. *J. Phys. Chem. A* **2001**, *105*, 8262.
(39) Koseki, S.; Ishihara, Y.; Umeda, H.; Fedorov, D. G.; Gordon, M. S. *J. Phys. Chem. A* **2002**, *106*, 785.
(40) Koseki, S.; Ishihara, Y.; Umeda, H.; Fedorov, D. G.; Schmidt, M. W.; Gordon, M. S. *J. Phys. Chem. A* **2004**, *108*, 4707.
(41) Schmidt, M. W.; Gordon, M. S. *Annu. Rev. Phys. Chem.* **1998**, *49*, 233.
(42) Lengfield,B. A., III; Jafri, J. A.; Phillips, D. H.; Bauschlicher, C. W., Jr. *J. Phys. Chem.* **1981**, *74*, 6849.
(43) Stevens, W. J.; Basch, H.; Krauss, M.; Jasien, P. *Can. J. Chem.* **1992**, *70*, 612.

(44) Cundari, T. R.; Stevens, W. J. *J. Chem. Phys.* **1993**, *98*, 5555.
(45) Koseki, S.; Matsushita, T.; Gordon, M. S. *J. Phys. Chem. A* **2006**, *110*, 2560.
(46) Exponents of 1.472 and 0.993 are used for *f* functions on Pd and Pt. The d exponents are 0.650 (S) and 0.800 (C and N).
(47) Becke, A. D. *J. Chem. Phys.* **1993**, *98*, 5648.
(48) Becker, D.; Yersin, H.; von Zelewsky, A. *Chem. Phys. Lett.* **1995**, *235*, 490.
(49) Yersin, H.; Schützenmeier, S.; Wiedenhofer, H.; von Zelewsky, A. *J. Phys. Chem.* **1993**, *97*, 13496.
(50) Schmidt, J.; Wiedenhofer, H.; von Zelewsky, A.; Yersin, H. *J. Phys. Chem.* **1995**, *99*, 226.
(51) Christine, C.-D.; von Zelewsky, A. *Inorg. Chem.* **1987**, *26*, 3354.
(52) Wiedenhofer, H.; Schützenmeier, S.; von Zelewsky, A.; Yersin, H. *J. Phys. Chem.* **1995**, *99*, 13385.
(53) Schmidt, M. W.; Baldridge, K. K.; Boatz, J. A.; Elbert, S. T.; Gordon, M. S.; Jensen, J. H.; Koseki, S.; Matsunaga, N.; Nguyen, K. A.; Su, S.; Windus, T. L.; Dupuis, M.; Montgomery, J. A., Jr. *J. Comput. Chem.* **1993**, *14*, 1347.
(54) Yamaguchi, T.; Yamazaki, F.; Ito, T. *J. Am. Chem. Soc.* **1999**, *121*, 7405.
(55) The energy barriers are calculated to be 4.1 (Pd) and 3.1 (Pt) kcal/mol for the corresponding optical isomerization on the potential energy surfaces of the ground state at the MCSCF+SOCI/SBKJC+p level of theory.
(56) Glasbeek, M.; Sitters, R.; van Veldhoven, E.; von Zelewsky, A.; Humbs, W.; Yersin, H. *Inorg. Chem.* **1998**, *37*, 5159.
(57) Colbert, D. T.; Miller, W. H. *J. Chem. Phys.* **1992**, *96*, 1982.
(58) Baldo, M. A.; O'Brien, D. F.; Thompson, M. E.; Forrest, S. R. *Phys. Rev. B* **1999**, *60*, 14422.
(59) Matsushita, T.; Asada, T.; Koseki, S. In preparation.